



APPLICATION OF DRY WORKING FLUIDS FOR THE EVALUATION OF SOLAR POWERED ORGANIC RANKINE CYCLE.

Diwa James Enyia¹, Dane Osim-Asu²

^{1,2}Department of Mechanical Engineering, Cross River University of Technology, Calabar, Nigeria.
Corresponding Author: enyiajames@yahoo.com

Abstract

This research encompasses a model to assess the performance of a solar-powered organic Rankine cycle (ORC). The system was assessed in two different cities, Maiduguri and Port Harcourt both in Northern and Southern part of Nigeria respectively, because of their different temperate zones, using five different dry organic working fluids, R123, R245ea, R236ea, R236fa, and R245fa. The aim of this research is to evaluate how hourly temperature change affects the electricity production and exergy destruction rates of the solar ORC, and to investigate the effect of the working fluid on the proposed system. The system was also assessed, to investigate the effect of average hourly outdoor temperatures on its performance. The potential of the system to reduce primary energy consumption and carbon dioxide emissions is also evaluated. Results show that the ORC produces the most electricity during the middle of the day, when the temperatures are the highest and when the solar collectors have the highest efficiency. Also, R236ea is the working fluid that shows the best performance of the evaluated fluids. An economic analysis was performed to determine the capital cost available for the proposed system, and it was discovered that the ORC in Port Harcourt had slightly higher savings of 8,308 kwh compared to 8,230 kwh of the Maiduguri region.

Keywords: Efficiency, Organic Rankine Cycle, Performance, Solar, Working Fluids.

CC Capital Cost

CDE Carbon Dioxide Emission

CFC chlorofluorocarbon

ECF Electricity Conversion factor

HCFC hydrochlorofluorocarbon

HVAC heat, ventilation and air conditioning

ORC Organic Rankine Cycle

PBP Pay Back Period

PEC Primary Energy Consumption

SCF Solar Conversion factor

medium-temperature heat sources [1]. ORCs can be implemented as power generating units for waste heat recovery systems, solar application, and geothermal applications since they generate power from low-temperature heat [2]. A relative small amount of electricity is produced from these applications; which means, ORCs are ideal for small-scale power generation applications. The selection of the organic fluid greatly affects the performance of ORCs; so, standards for selecting fluid and performance have been widely studied [3]. The ORC is one of the various technologies presented as alternative to photovoltaic PV for the conversion of solar irradiation to electrical energy. The conventional Rankine cycle and the ORC has similar operating

1.0 Introduction

Organic Rankine Cycles (ORCs) are Rankine cycles that uses an organic working fluid instead of water. Organic fluids are utilized so that the ORC can generate electricity from low- and

principles, but in this case with the use of organic compound rather than water as its working fluid. This has been employed for conversion of heat from low-to-medium temperature sources such as biomass, process waste heat and geothermal, having the system operating mostly with little maintenance requirement for couples of decades now [4].

Solar radiation is used to heat and evaporate the working fluids at high pressure in solar powered ORC, afterwards, the vapour is expanded to generate mechanical shaft work, which can be applied directly as mechanical work, to drive a pump or through a generator to produce electrical power. The ambidexterity of the output and capability to accumulate solar heat such as hot water, presents possible advantage ahead of solar PV home heat and load profile of electricity matching. In addition, the possibility to create high-electricity, low-cost components worthy for the home scale could see enhanced competitiveness with PV in the short-term [5]. The technology of ORC is properly placed all over the world with so many commercial systems in operation. The size ranges from micro in kw to as high as 10MW output of electric power for a wide range of operating temperature and working fluids [6]. Most of these systems incorporate turbines as the expansion device that tends to operate at high rotational speeds and mostly suited for larger scale system with higher shaft output power >10kw. Some non-commercial systems have used acquired scroll-compressors run to upset as the expansion device far out <10kw [7,8]. An example of solar ORC in operation is a 1MW_e concentrating solar power with a collector field area in excess of 10,000m² [9], and an experimental 2.5kw solar reverse osmosis desalination system with non-concentration evacuation-tube collector array of area 88m² [10].

In reality, reciprocating expanders, with their simple and rugged construction, and advanced state of development, can be produced at low cost and with high reliability, and are capable to operate with high efficiency at low power output [11].

The ORC emergence in this research is due to its *technical advantages* which includes; High Cycle Efficiency, Very High Turbine Efficiency, Low Turbine Mechanical Stress, due to low peripheral stress, Low turbine RPM, allowing the direct drive of the electric generator without gear reduction in many application, and No erosion of blades, thanks to the absence of moisture in the vapour nozzles, and also its *Operational advantages* which includes; Simple start-stop procedures, Automatic and continuous operation, No operator attendant needed, High availability, typically 98%, High efficiency at partial load, Lower maintenance cost, Quiet operation, and Long life.

Epileptic power supply and very high tariffs from the grid has led to research findings of alternative and cost effective means of power generation and supply to consumers, which in this research case involve using ORC with 5 different working fluids.

Although previous work has been done in the solar ORC area, the objective of this paper is to further investigate the performance of a solar-powered ORC that uses a two-axis tracking flat-plate solar collector instead of an evaporator in the ORC system. The author applied five different dry working fluids which includes; R123, R245ea, R236ea, R236fa, and R245fa to determine the performance of the solar-powered ORC. The radiation data is based on the latitude of the location, while the ambient temperature data is determined by the location. The output power produced, the total exergy destruction, and the rate of mass flow required for the system is investigated every hour for a representative day for every month in the year. The outdoor temperature effect on the performance of the ORC is evaluated by modeling the ORC in two locations (Maiduguri and Port Harcourt) with the close latitude but different climate conditions. The effects of using a solar ORC on primary energy consumption (PEC) and carbon dioxide emission (CDE) was also researched to

investigate if savings occur when compared to acquiring electricity from the grid. More so, the effects of the area of solar collector, pressure of the solar collector, and temperature of the condenser on the overall ORC performance is determine with the help of a parametric study analysis.

2.0 Literature Review

Several studies have been performed for various ORC applications, [11] uses micro turbines in 16 various locations to investigate the performance comparison of combined micro-turbines and ORCs. It was discovered that for some locations where the use of a micro-turbine was not of good value, the combination of a micro-turbine and an ORC was a feasible option to grid power. Madhawa et al [12] performed an economic optimization for a waste heat ORC and combined the economic optimization with a thermal optimization based on the maximum net power output. Chang et al [13] uses economic measures to determine the off-design performance of a solar-powered ORC and optimized the design parameters of the heat exchangers. Gao et al [14] applied the use of the ratio of area of heat transfer to net power by optimizing a geothermal ORC. Four different working fluids were applied in the simulation and it was discovered that based on the chosen measures, ammonia was investigated to be the most viable fluid of all four studied. Srivinasan et al [15] studied the performance of scroll expanders in an ORC using experimental and computational fluid dynamics methods. Scrinivasan et al [16] used thermodynamic and heat transfer models to simulate an ORC, two different scroll expanders, and compared the results to experimental data. [17, 18] determined the possibility of using ORC with the exhaust waste heat recovery from a dual-fuel low-temperature combustion engine. They found that the engine fuel conversion efficiency was improved by an average of 7%, while NO_x and

CO₂ emissions recorded an average of 18% decrease.

SCF Solar Conversion factor. Several studies have investigated the reduction in PEC and CDE using alternative systems. Fang et al [19] carried out a combined cooling heat and power (CCHP) analysis for a building to investigate the required operating conditions to have primary energy savings. Bu et al [20] studied a combined heating and power (CHP) system coupled with an ORC. The total PEC, cost, and CDE of a CHP-ORC with a CHP system for buildings located in various climate zones were analyzed and compared. They found that using a CHP-ORC resulted in a reduction in PEC, cost, and CDE when compared to a CHP system; however, the benefits of using a CHP-ORC depended on the building's location. Fang [21] compared a CCHP system with a CCHP-ORC and determined that the studied CCHP- ORC system provided greater savings in PEC, operational cost, and CDE than a CCHP system located in the city of Beijing.

Using solar-powered ORCs has previously been studied [22-24]. Wang et all [25] apply the use of TRNSYS to simulate a residential or commercial building with solar power to heat water and produce work using an ORC. A comparison of about 11 various fluids were made to investigate which of the combinations produced optimal result for the modeled building [26] uses parabolic trough solar collectors and R134a as the working fluid to simulate a solar geothermal hybrid ORC plant. The net power was determined by performing an hourly simulation for four various locations. The economic analysis involved was also investigated. Wang [27] uses a compound parabolic concentrator solar collector in line with the ORC, instead of applying an evaporator to combine geothermal energy and solar energy as heat sources for an ORC. They used R134a, R236fa, and R245fa as their working fluids in the investigation. Results output were presented for every hour in each

standard day between December and January. The generated heat from the solar collectors was stored in a heat storage tank in order to control the power output. The heat storage tank was connected to an evaporator in order to transfer the heat to the ORC. The working fluids used for this study were R123 and R245fa. The results for incident solar flux, power output, water temperature in the heat storage tank, and ambient temperature were reported hourly over a day. A sensitivity analysis was also carried out to study the effects of the turbine inlet temperature and pressure and the condensation temperature on the ORC.

It is from this knowledge gap the author of the current paper intend to fit in to solve the identified gap. It will involve the use of five different dry organic working fluids namely R123, R245ea, R236ea, R236fa, and R245fa to evaluate solar-powered ORC.

3.0 Research Methodology

The proposed model that was employed to simulate the performance of a solar-powered

ORC is presented in this session. Figure 1(a) illustrates a schematic of the solar-powered ORC to be used in this research and Figure 1(b) shows the corresponding $T-s$ diagram for the proposed modeled solar-powered ORC. The major four components applied for use in a basic ORC are as follows: a pump, an evaporator, a turbine, and a condenser. The pump increases the pressure of the organic working fluid before the evaporator, which in this case is the solar collector.

The solar collector transfers heat to the organic working fluid using solar energy. The fluid then enters the turbine at high pressure and temperature and exits at a lower temperature and pressure, producing power. Finally, the organic working fluid enters the condenser where heat is transferred from the working fluid to a low temperature sink. This condenses the fluid to a liquid at the initial temperature of fluid as it enters the pump, thus starting the cycle again. The proposed system was simulated by using dry fluids since it has been proven that they provide better performance than wet fluids for ORC applications [6].

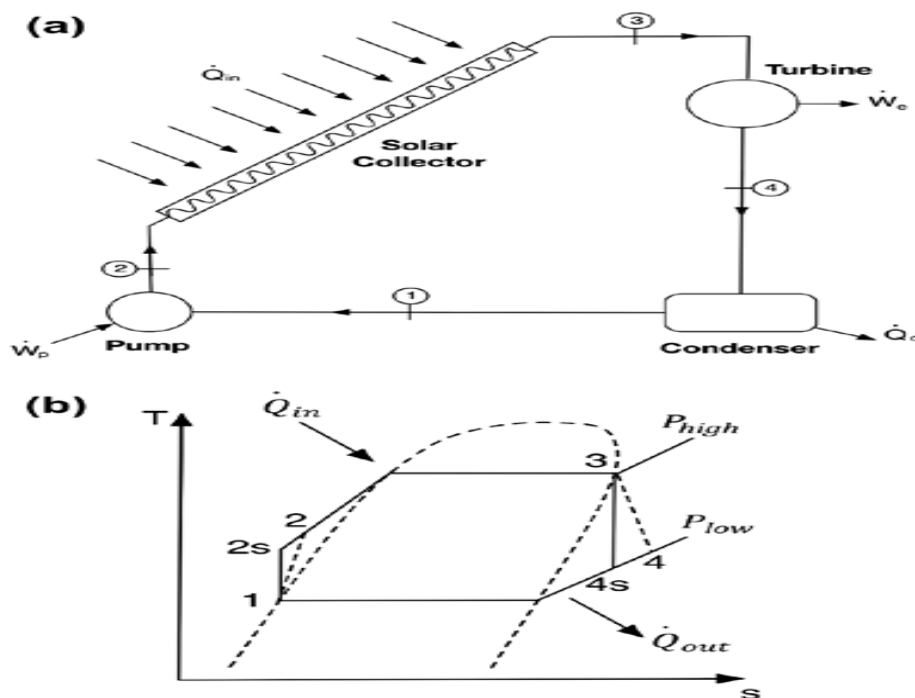


Figure 1: (a) Schematic of the proposed solar powered ORC (b) Temperature-entropy diagram of the proposed system.

The **pump power** can be expressed as: process 1-2.

$$W_p = \frac{W_{ps}}{\eta_p} = \frac{m_{ORC}(h_{2s}-h_1)}{\eta_p} = m_{ORC}(h_2 - h_1) \dots \dots \dots (1)$$

where W_{ps} is the ideal power of the pump, m_{ORC} is the mass flow rate of the working fluid, η_p is the pump isentropic efficiency, and h_1 , h_{2s} , and h_2 are the enthalpies of the organic working fluid at the inlet, outlet of the pump for the ideal case, and outlet of the pump for the real case, respectively.

The exergy destruction rate of the pump is given by

$$\Pi_p = E_p - (E_2 - E_1) \dots \dots \dots (2)$$

where E_2 and E_1 are the exergy rates at States 2 and 1, and E_p is exergy of the pump. The change in exergy from state 1 to state 2 is:

$$E_2 - E_1 = m_{ORC}(h_2 - h_1 - T_0(s_2 - s_1)) \dots \dots \dots (3)$$

Where T_0 , s_2 , and s_1 are the temperatures at the dead state of 298K in this model and the entropy values at states 2 and 1. The exergy transfer of the pump is:

$$E_p = W_p \dots \dots \dots (4)$$

Process 2-3, Solar collector: This is a constant-pressure transfer of heat process. The solar collector heats the working fluid at the pump outlet to the turbine inlet condition. The heat transfer rate from the solar collector into the working fluid is given by:

$$Q_e = Q_{in} = m_{ORC}(h_3 - h_2) \dots \dots \dots (5)$$

where h_3 and h_2 are the enthalpies of the organic working fluid at the exit and inlet of the solar collector, respectively.

The **turbine power** is given by: Process 3-4

$$W_t = W_{ts}\eta_t = m_{ORC}(h_3 - h_{4s})\eta_t = m_{ORC}(h_3 - h_4) \dots \dots \dots (6)$$

where W_{ts} is the ideal power of the turbine, η_t is the turbine isentropic efficiency, and h_{4s} and h_4 are the enthalpies of the organic working fluid at the outlet of the turbine for the ideal case and for the real case, respectively. The turbine exergy destruction rate is:

$$\Pi_t = E_3 - E_4 - E_t \dots \dots \dots (7)$$

The change in exergy from state 3 to state 4 is given by:

$$E_3 - E_4 = m_{ORC}(h_3 - h_4 - T_o(s_3 - s_4)) \dots (8)$$

Where E_4 is the exergy rate at state 4 and s_4 is the entropy at state 4.

The turbine exergy is;

$$E_t = W_t \dots \dots \dots (9)$$

The **condenser heat** rate can be expressed as: Process 4-1, condenser

$$Q_c = Q_{out} = m_{ORC}(h_1 - h_4) \dots \dots \dots (10)$$

The exergy destruction rate is given by the following equation;

$$\Pi_c = E_4 - E_1 - E_{QC} \dots \dots \dots (11)$$

The exergy rate from state 4 to state 1 is;

$$E_4 - E_1 = m_{ORC}(h_4 - h_3 - T_o(s_4 - s_1)) \dots \dots (12)$$

The exergy of the container;

$$E_{QC} = Q_c \left(1 - \frac{T_0}{T_1}\right) \dots \dots \dots (13)$$

Where T_L is the low temperature heat sink which is assumed to be 303K

The **net power** generated by the ORC can be expressed as:

$$W_{net} = W_t - W_p \dots \dots \dots (14)$$

The **thermal efficiency** is defined as the ratio between the net power of the cycle to the heat input rate as follows:

$$\eta_{th} = \frac{W_{net}}{Q_{in}} = \frac{(h_3 - h_4) - (h_2 - h_1)}{h_3 - h_2} \dots \dots \dots (15)$$

The exergy efficiency for ORC can be expressed as;

$$\eta_x = \frac{E_{W_{net}}}{E_{Q_{in}}} \dots \dots \dots (16)$$

Where $E_{W_{net}}$ and $E_{Q_{in}}$ are the exergy of the products and exergy input to the ORC. $E_{W_{net}}$ can be estimated as;

$$E_{W_{net}} = W_{net} \dots \dots \dots (17)$$

PEC Savings: This is necessary since the solar energy would replace electricity. The equation below is used to determine the PEC savings in this study;

$$PEC_{savings} = W_{net}ECF_{PEC} - W_{net}SCF_{PEC} \dots (18)$$

Where $PEC_{savings}$ is the primary energy consumption savings, the electricity conversion factor for primary energy consumption is given as ECF_{PEC} and the solar conversion factor for the primary energy consumption is SCF_{PEC} , its assumed to be 1 in this study.

Carbon dioxide emission reduction: There is no emission from ORC, as such, reducing the purchased electricity from the grid, will reduced CDE. The location of the grid greatly affects the amount of CDE produced from electricity generation. The equation below is used to determine the amount of CDE produced from using an on-site solar ORC.

$$CDE_{reduction} = W_{net}ECF_{CDE} \dots \dots \dots (19)$$

Where $CDE_{reduction}$ is the reduction in CDE and ECF_{CDE} is the electricity conversion factor for CDE.

Cost savings and available capital cost: it is required to investigate the cost savings from the electricity generation in other to determine the available capital cost CC. The cost savings from generating electricity is determined as;

$$Savings = W_{net}Cost_e \dots \dots \dots (20)$$

Where $Cost_e$ is the cost of electricity for the various locations. Multiplying the savings by the payback period will determine the maximum available CC to achieve the desired payback period. The available CC can be;

$$CC = Savings (PBP) \dots \dots \dots (21)$$

Where PBP is the desired payback period.

4.0 Results analysis and discussion

The research outcome represents an hourly solar ORC which is modeled and evaluated using five different dry organic working fluids to determine the consequence of ambient temperature and working fluid on the system. A comparison of 5 different dry organic fluids were used in the simulation namely; R123, R245ea, R236ea, R236fa, and R245fa, for the ORC. The condensing temperature was assumed to 32⁰C, while the system high pressure was taken to be 2MPa for all the fluids to be compared. The pressure and temperature ranges for each of the

evaluated fluids obtained using REFPROP7 software. The system was further evaluated with the use of four collectors with an area of about 3.696m² each to study the performance of the proposed solar ORC. The solar energy generated by the solar ORC for each representative day for each month of the evaluated fluids is as shown in figure 2. The outcome reveals that when the ORC uses R236ea, it generates the highest net energy for each day during the month for the whole year. On the other hand, when the ORC uses R123, it indicates the lowest performance amongst the evaluated fluids.

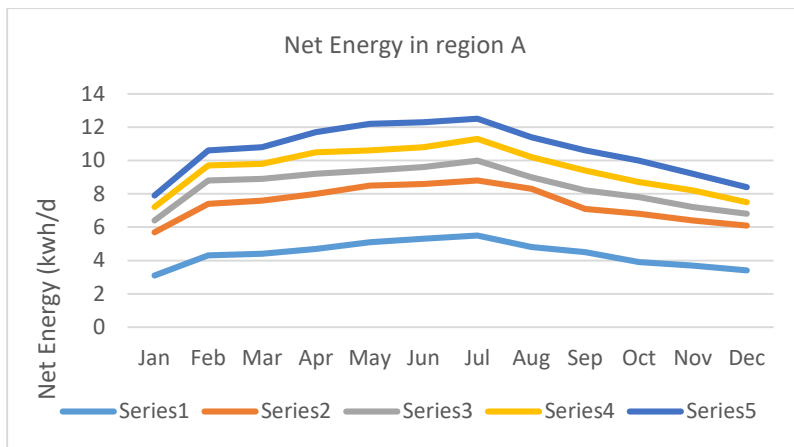


Figure 2: Net energy generated per representative day in Zone A for each working fluids.

The total energy destroy by the ORC per representative day for each month for all the evaluated fluids is as shown in figure 3. Less energy is destroyed per day under the evaluated condition when the system uses R236ea, while

on the other hand, more energy is destroyed when the system uses R123. The results in figure 2 and 3 clearly shows that when the system destroyed less exergy, it performs better as shown by higher thermal and exergy efficiencies.

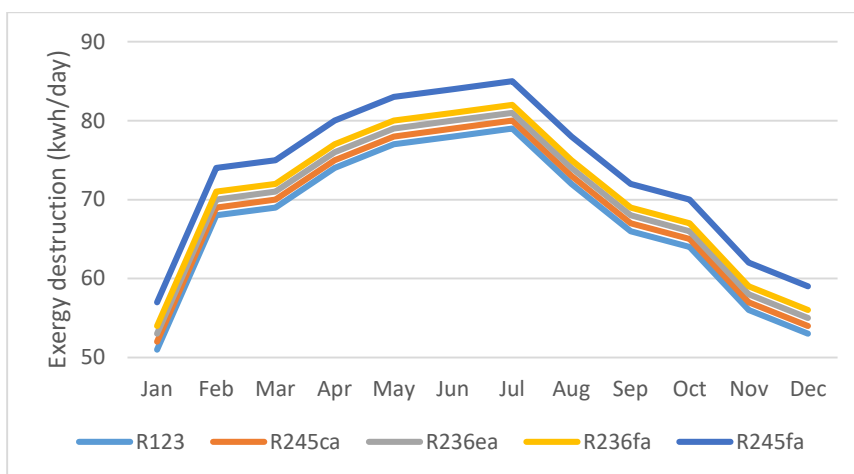


Figure 3: Total energy destroyed per representative day in Zone A for each of the modeled fluids.

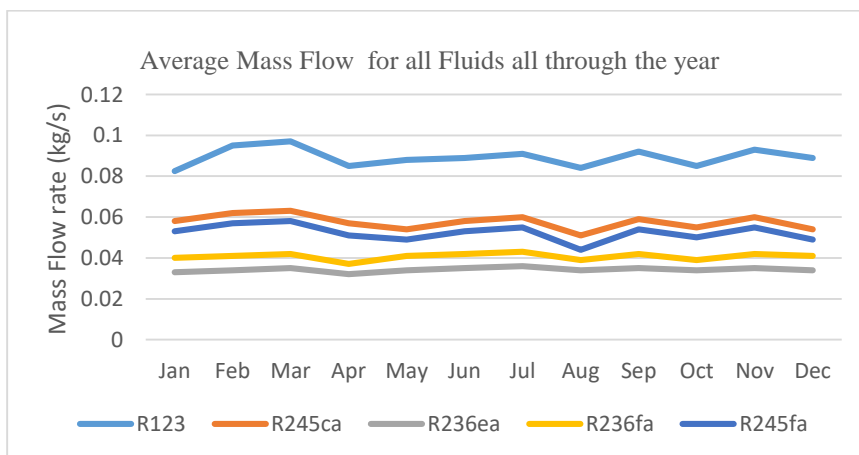


Figure 4: Average mass flow rate for each representative day of the month for each of the fluids modeled for Zone A.

The required average mass flow rates for each representative day for the results presented in figure 2 and 3 are as shown in figure 4. The figure shows that the average mass flow rate fluctuates within a range for the different months of the year.

The ORC operating with R123 requires the highest rate of mass flow, while the ORC operating with R236ea requires the lowest rate of mass flow. The outcome in figures 2 to 4 shows that R235ea yields the highest net energy with the lowest amount of exergy destroyed and lowest mass flow rate. In the same way, R236ea and R123 are the working fluids with the second lowest and highest volumetric flow rate entering

the expander respectively. This means, if the pump cost and the expander cost are estimated based on the proposed model by Quoilin et al [10], R236ea is the working fluid with the lowest pump and second lowest expander costs, while R123 is the working fluid with the highest pump and expander costs. It can be seen in figure 5, the net energy produced per month by each fluid. The net energy for each month was estimated by the net energy produced in a representative day of the month multiplied by the number of days in the month. The outcome shows that R236ea produced the most net energy each month when compared to the other four fluids in the study, while R123 produced the lowest. This also explains that the solar powered ORC is able to generate most energy during the spring and summer months, having the peak generation in the month of July for all evaluated fluids.

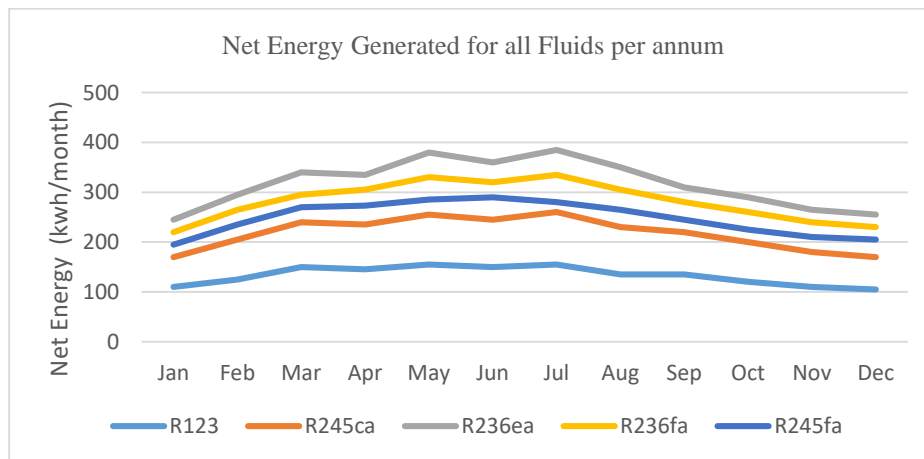


Figure 5: Net energy generated per month in Zone A for each of the modeled fluids.

The total yearly generated energy for each of the evaluated cases is presented in figure 5, the highest net energy is produced by the ORC using

R236ea as the working fluids (3,888 kwh/yr), while the lowest is produced by the ORC using R123 (1,625.kwh/yr).

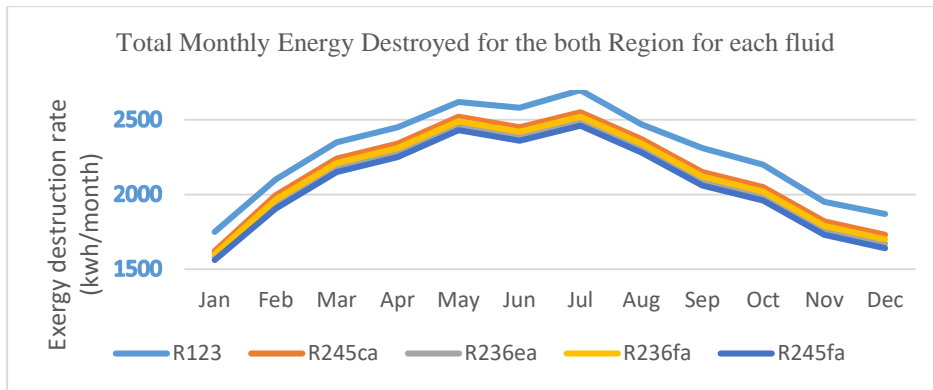


Figure 6: Total energy destroyed per month in both zones for each of the modeled fluids.

The figure 6 indicates the total exergy destroyed per month for all fluids in the study. In the same way, the total exergy destroyed per month was estimated by multiplying the calculated total exergy destroyed per representative day of the month by the number of days in the month. Also, the results show that R236ea destroys the least amount of exergy, while R123 destroys the most. This implies that it can be observed how the selected fluids plays a very vital role in the performance of the ORC since the ORC using R236ea was able to generate about 139% more energy compared to using R123, while also allowing 8% less exergy destruction. More so, R236ea has the highest energy generated and the lowest amount of exergy destroyed per day and year and the lowest mass flow rate required under the evaluated conditions. This implies that R236ea is used as the working fluid for the results that are presented in this research.

To show the performance of the system in different seasons, the solar ORC was assessed in Zone A for 28 January and July using R236ea as the working fluid. The ORC was modeled in two locations with the same latitude but different climate conditions, Zone A (Portharcourt) and Zone B (Maiduguri), this is to evaluate the effect of average hourly outdoor temperatures on the ORC performance. The solar irradiation values are the same for both cities since they have roughly the same latitude, but average hourly temperature vary per location since they are located in different climate zones. The net energy and total exergy generated per month by the ORC for both locations is as shown in figure 7. The comparison depicts that Zone B generated a slightly higher energy and exergy for each month by the ORC except 28 February and July. The total energy generated in Zone B was about 3,985 kwh/yr. which is 3.1% higher than the energy generated in Zone A.

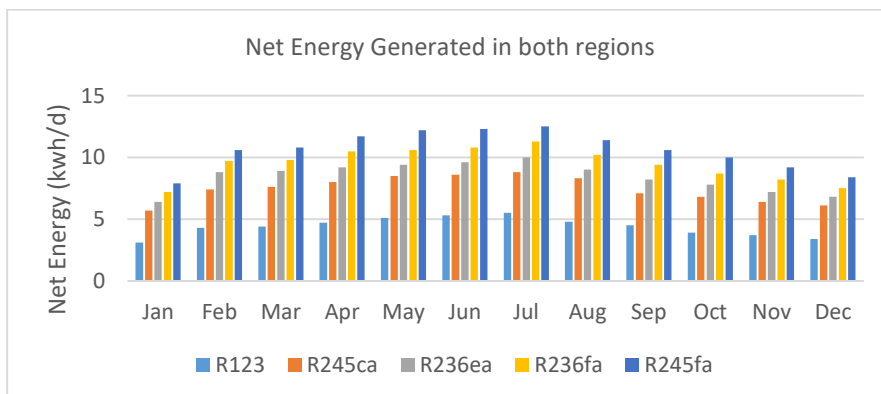


Figure 7: The net energy generated and total exergy destroyed per month for both zones.

Carbon dioxide Emission (CDE) and Primary Energy Consumption (PEC).

The investigation also includes finding the effect of replacing purchased electricity from the grid with the electricity generated by the ORC. Since the electricity from the ORC is generated from solar energy on site, the SFC_{PEC} has a value of 1. The conversion factor for electricity purchase vary from state to state, and for the two states Borno (Maiduguri) and Rivers (Port Harcourt) involved in this study, the EFC_{PEC} values are 3.35 and 3.27 respectively. Figure 8 indicates possible monthly PEC savings for both zones. The total

PEC savings for both zones are 8, 297 and 8, 219 kwh/yr respectively.

In a similar way, using a solar powered ORC top generate on-site electricity from the grid, both zones have an ECF_{CDE} value of 0.471 and 0.538 kg/kwh, respectively. The possible CDE monthly savings are as shown in figure 4.8. The total CDE savings for both zones are 1, 817 and 2, 138 kg/yr respectively. We can conclude that the solar powered ORC not only generate power but also reduce the amount of PEC and CDE as compared with electricity production in a power plant.

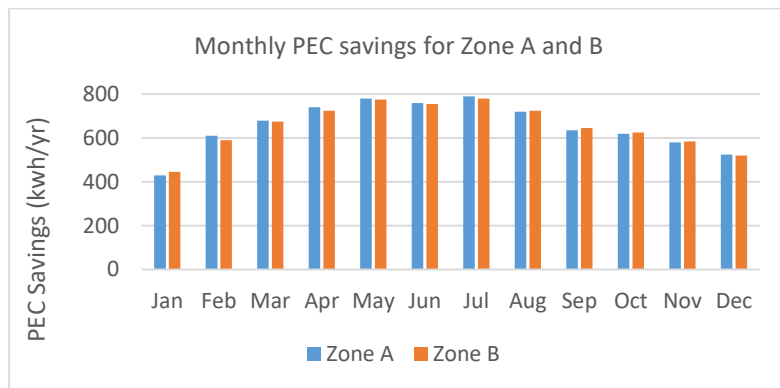


Figure 8: Monthly PEC savings for both zones

The possible economic savings produced by the ORC are investigated by comparing the chosen working fluids in both zones, in addition, the maximum capital cost was investigated for various payback periods for each of the fluids. The cost of average electricity for both zones are 0.1108 and 0.1161 \$/kwh respectively, which was determined with the use current electricity data for residential consumers (Monthly electric power consumed for the period. The capital cost for both zones also shows that R236ea has the

highest available, while R123 has the lowest available capital cost for both zones. The solar ORC Zone B (Maiduguri) has higher values for all fluids when compared to the solar ORC in Port Harcourt. This can be explained since more electricity is generated in Maiduguri which is addition has slightly higher electricity cost. The capital cost for R236ea in Maiduguri given a 10year payback period, is approximately \$4, 624 compared to \$4, 288 in port Harcourt, with the same payback period.

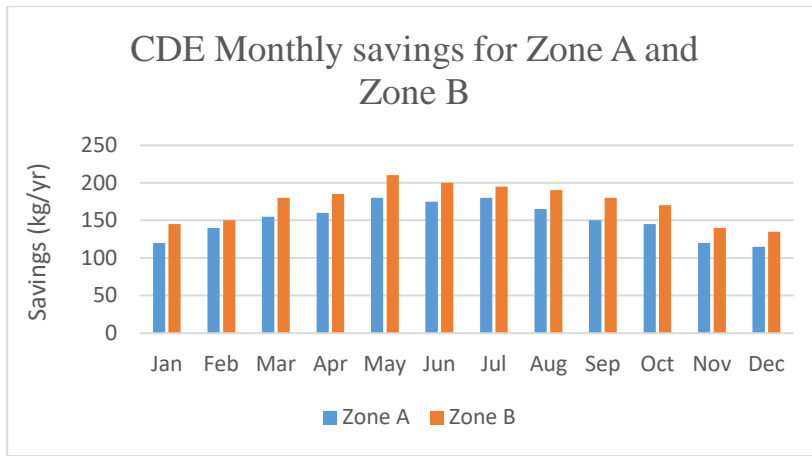


Figure 9: Monthly CDE savings for both zones

Hourly trends are compared for a given period. The possibility for PEC and CDE savings is also studied when replacing purchased electricity with on-site ORC generated power. More so, a parametric study is carried out to investigate the effect of the temperature and pressure of the organic working fluids and the solar collector area on the electricity production in the solar ORC. For all of the evaluated fluids, the model will be able to show that the when ORC produced the most net power over the months. The working fluid with the most energy, highest thermal efficiency, and exergetic efficiency will be determined. The fluid with the lowest exergy destruction rate and lowest average mass flow rate will be determined. The fluid with the highest capital cost available and lowest pump power required, and lowest volumetric flow rate into the expander will be determined.

Conclusions

This research showcased an hourly solar ORC which was modeled and assessed in two different temperate zones namely; Maiduguri (Borno), and Port Harcourt (Rivers), with the application of five different dry organic working fluids to investigate the effect of ambient temperature and working fluid on the system. The hourly trends were compared for the months of January and July. The possibility for PEC and CDE savings was also studied when replacing purchased electricity with on-site ORC-generated power. For all of the assessed fluids, the model showed

that the ORC produced the most net power during the raining and dry season months.

Out of the five fluids assessed, R236ea performed the best from the study under the modeled conditions. It generated the most net energy per year of about 3,888 kWh/year, had the highest thermal efficiency and exergetic efficiency, and had the lowest rate of exergy destruction as well as the lowest average mass flow rate required. The lowest pump power required, as well as the highest capital cost was found to be R236ea, and it is also the second lowest volumetric flow rate into the expander, which indicates that R236ea indicates the most promise for economic viability among the selected fluids. This implies that R236ea was the modeled working fluid for the remainder of the study. While determining the effect of hourly irradiation and changes in temperature, it was investigated that the highest net energy produced and highest total exergy destroyed occurred during the middle of the day, when the solar irradiation was the highest. The mass flow rate followed the same hourly trend as the net energy produced. These trends were seen in both the months of January and July. The efficiency trend of the solar collector, however, differed from January to July. In January, efficiency of the the solar collector was almost constant but peaked during the middle of the day. However, in July, the efficiency of the solar collector peaked at the end of the day. The exergy analysis investigated

that the solar collector was the highest contributor to the total exergy destruction.

The solar ORC was modeled in Maiduguri and Port Harcourt to compare the performances because the cities are in different temperate zones. Therefore, the same solar irradiation data were used, but the ambient temperatures for the two cities differ. In general, Maiduguri had the higher hourly ambient temperatures which affected the solar efficiency. This led to a slightly higher net energy produced for most months as well as slightly higher average mass flow rates for most months. The amount of PEC and carbon dioxide emission savings was evaluated for the two cities as well. While the ORC in Maiduguri produced more electricity than in Port Harcourt resulting in less electricity purchased from the grid, the ORC in Port Harcourt had slightly higher PEC savings, 8,308 compared to 8,230 kWh. This is as a result of the fact that the ECF_{PEC} value was higher in Port Harcourt than Maiduguri. The ORC in Maiduguri had greater carbon dioxide savings than in Port Harcourt which corresponds to the higher ECF_{CDE} value.

Therefore, in this case, where the net energy produced is very similar between the two cities, the city with the higher electricity conversion factor has the possibility for greater savings.

As the solar collector pressure increased, the Net-work increased, while the total exergy destroyed and the average mass flow rate decreased, but the effect of the pressure on the Net-work, the total exergy destroyed, and average mass flow rate decreases as the pressure approaches the critical pressure for the fluid. The condensing temperature has an inverse effect on the net energy produced, the total exergy destroyed, and the mass flow rate. Reducing the turbine efficiency reduced the net energy produced and slightly increased the total exergy destroyed. Varying the solar collector pressure and the condensing temperature affected both the thermal and exergetic efficiencies, while the number of solar collectors did not. The highest

efficiencies in this study occur at a high solar collector pressure and a low condensing temperature. The performance on the assessed fluids corroborates this as well. R236ea, which had the highest pressure ratio and temperature range, is the fluid that shows the best performance among the evaluated fluids under the modeled conditions.

Acknowledgement

The authors wish to most profoundly appreciate Tertiary Education Trust Fund TETFUND for her benevolence in sponsoring this research work all through. We are really most grateful from the debt of our hearts.

References

- [1] Bao, J., & Zhao, L. (2013). A review of working fluid and expander selections for organic Rankine cycle. *Renewable and Sustainable Energy Reviews*, 24, 325–342. <http://dx.doi.org/10.1016/j.rser.2013.03.040>
- [2] Hung, T., Wang, S., Kuo, C., Pei, B., & Tsai, K. (2010). A study of organic working fluids on system efficiency of an ORC using low-grade energy sources. *Energy*, 35, 1403–1411. <http://dx.doi.org/10.1016/j.energy.2009.11.025>
- [3] Lakew, A. A., & Bolland, O. (2010). Working fluids for low- temperature heat source. *Applied Thermal Engineering*, 30, 1262–1268.
- [4] James Freeman, Klaus Hellgardt, Christos N. Markides.,(2015). An assessment of solar-powered organic Rankine cycle systems for combined heating and power in UK domestic applications. *Applied Energy* 138 (2015) 605–620
- [5] Markides CN. (2013). ‘The role of pumped and waste heat technologies in a high- efficiency sustainable energy future for the UK. *Appl Therm Eng* 2013;53(2): 197–209.
- [6] Vélez F, Segovia JJ, Martín MC, Antolín G, Chejne F, Quijano A. A technical, economical and market review of organic Rankine cycles for

the conversion of low-grade heat for power generation. *Renew Sustain Energy Rev*;16(6): 4175–89.

[7] Quoilin S, Orosz M, Hemond H, Lemort V. (2011). Performance and design optimization of a low-cost solar organic Rankine cycle for remote power generation. *Sol Energy* ;85(5):955–66.

[8] Manolakos D, Kosmadakis G, Kyritsis S, Papadakis G.(2009). On site experimental evaluation of a low-temperature solar organic Rankine cycle system for RO desalination. *Sol Energy* ;83(5):646–56.

[9] Canada S, Cohen G, Cable R, Brosseau D, Price H.(2004). Parabolic trough organic Rankine cycle solar power plant. In: DOE solar energy technologies program review meeting. USA: Denver.

[10] Quoilin, S., Declaye, S., Tchanche, B. F., & Lemort, V. (2011). Thermo-economic optimization of waste heat recovery organic Rankine cycles. *Applied Thermal Engineering*, 31, 2885–2893. <http://dx.doi.org/10.1016/j.applthermaleng.2011.05.014>

[11] Calise, F., Capuozzo, C., Carotenuto, A., & Vanoli, L. (2014). Thermo-economic analysis and off-design performance of an organic Rankine cycle powered by medium- temperature heat sources. *Solar Energy*, 103, 595–609. <http://dx.doi.org/10.1016/j.solener.2013.09.031>

[12] Madhawa Hettiarachchi, H. D., Golubovic, M., Worek, W. M., & Ikegami, Y. (2007). Optimum design criteria for an organic Rankine cycle using low-temperature geothermal heat sources. *Energy*, 32, 1698–1706. <http://dx.doi.org/10.1016/j.energy.2007.01.005>

[13] Chang, J.-C., Chang, C.-W., Hung, T.-C., Lin, J.-R., & Huang, K.-C. (2014). Experimental study and CFD approach for scroll type expander used in low-temperature organic Rankine cycle. *Applied Thermal Engineering*, 73, 1444–1452.

[14] Gao, P., Jiang, L., Wang, L. W., Wang, R. Z., & Song, F. P. (2015). Simulation and experiments on an ORC system with different

scroll expanders based on energy and exergy analysis. *Applied Thermal Engineering*, 75, 880–888.

<http://dx.doi.org/10.1016/j.applthermaleng.2014.10.044>

[15] Srinivasan, K., Mago, P. J., Zdaniuk, G. J., Chamra, L. M., & Midkiff, K. C. (2008). Improving the efficiency of the advanced injection low pilot ignited natural gas engine using organic Rankine cycles. *Journal of Energy Resources Technology*, 130, 022201. <http://dx.doi.org/10.1115/1.2906123>

[16] Srinivasan, K. K., Mago, P. J., & Krishnan, S. R. (2010). Analysis of exhaust waste heat recovery from a dual fuel low temperature combustion engine using an organic Rankine cycle. *Energy*, 35, 2387–2399. <http://dx.doi.org/10.1016/j.energy.2010.02.018>

[17] Fumo, N., & Chamra, L. M. (2010). Analysis of combined cooling, heating, and power systems based on source primary energy consumption. *Applied Energy*, 87, 2023–2030. <http://dx.doi.org/10.1016/j.apenergy.2009.11.014>

[18] Mago, P. J., Hueffed, A., & Chamra, L. M. (2010). Analysis and optimization of the use of CHP-ORC systems for small commercial buildings. *Energy and Buildings*, 42, 1491–1498. <http://dx.doi.org/10.1016/j.enbuild.2010.03.019>

[19] Fang, F., Wei, L., Liu, J., Zhang, J., & Hou, G. (2012). Complementary configuration and operation of a CCHP- ORC system. *Energy*, 46, 211–220. <http://dx.doi.org/10.1016/j.energy.2012.08.030>

[20] Bu, X., Li, H., & Wang, L. (2013). Performance analysis and working fluids selection of solar powered organic Rankine-vapor compression ice maker. *Solar Energy*, 95, 271–278. <http://dx.doi.org/10.1016/j.solener.2013.06.024>

[21] Wang, J. L., Zhao, L., & Wang, X. D. (2010). A comparative study of pure and zeotropic mixtures in low- temperature solar Rankine cycle. *Applied Energy*, 87, 3366–3373. <http://dx.doi.org/10.1016/j.apenergy.2010.05.016>

- [22] Rayegan, R., & Tao, Y. X. (2013). Optimal collector type and temperature in a solar organic Rankine cycle system for building-scale power generation in hot and humid climate. *Journal of Solar Energy Engineering*, 135, 011012.
- [23] Astolfi, M., Xodo, L., Romano, M. C., & Macchi, E. (2011). Technical and economic analysis of a solar-geothermal hybrid plant based on an organic Rankine cycle. *Geothermics*, 40, 58–68.
<http://dx.doi.org/10.1016/j.geothermics.2010.09.009>
- [24] Tempesti, D., Manfrida, G., & Fiaschi, D. (2012). Thermodynamic analysis of two micro CHP systems operating with geothermal and solar energy. *Applied Energy*, 97, 609–617.
<http://dx.doi.org/10.1016/j.apenergy.2012.02.012>
- [25] Wang, X., Zhao, L., Wang, J., Zhang, W., Zhao, X., & Wu, W. (2010). Performance evaluation of a low- temperature solar Rankine cycle system utilizing R245fa. *Solar Energy*, 84, 353–364.
<http://dx.doi.org/10.1016/j.solener.2009.11.004>
- [26] Marion, M., Voicu, I., & Tiffonnet, A. L. (2012). Study and optimization of a solar subcritical organic Rankine cycle. *Renewable Energy*, 48, 100–109.
<http://dx.doi.org/10.1016/j.renene.2012.04.047>
- [27] Wang, M., Wang, J., Zhao, Y., Zhao, P., & Dai, Y. (2013). Thermodynamic analysis and optimization of a solar- driven regenerative organic Rankine cycle (ORC) based on flat-plate solar collectors. *Applied Thermal Engineering*, 50, 816–825.
<http://dx.doi.org/10.1016/j.applthermaleng.2012.08.013>